ORIGINAL ARTICLE

Throughput maximization for underlay CR multicarrier NOMA network with cooperative communication

Thirunavukkarasu Manimekalai | **Sparjan Romera Joan** (ID) | **Thangavelu Laxmikandan**

Department of ECE, College of Engineering Guindy, Anna University, Chennai, India

Correspondence
Sparjan Romera Joan, Department of ECE, College of Engineering Guindy, Anna University, Chennai, India.
Email: 20srjoan06@gmail.com

The non-orthogonal multiple access (NOMA) technique offers throughput improvement to meet the demands of the future generation of wireless communication networks. The objective of this work is to further improve the throughput by including an underlay cognitive radio network with an existing multi-carrier NOMA network, using cooperative communication. The throughput is maximized by optimal resource allocation, namely, power allocation, subcarrier assignment, relay selection, user pairing, and subcarrier pairing. Optimal power allocation to the primary and secondary users is accomplished in a way that target rate constraints of the primary users are not affected. The throughput maximization is a combinatorial optimization problem, and the computational complexity increases as the number of users and/or subcarriers in the network increases. To this end, to reduce the computational complexity, a dynamic network resource allocation algorithm is proposed for combinatorial optimization. The simulation results show that the proposed network improves the throughput.

KEYWORDS
CDRT, cooperative relaying, Multi-carrier NOMA, throughput, underlay CRN

1 | INTRODUCTION

The compounding growth of mobile wireless devices and ubiquitous computing has raised an indispensable need to develop robust transmission techniques that optimize spectrum utilization. To meet this requirement, researchers are exploring the domains of massive multiple-input, multiple-output (massive MIMO), small cells, device-to-device communication, cooperative relaying, spectrum sharing, and novel multiple access schemes. Under current standards, orthogonal multiple access (OMA) schemes such as frequency domain multiple access (FDMA), time division multiple access, code division multiple access, and orthogonal FDMA (OFDMA) have been used in wireless cellular networks to serve multiple users. Although these multiple access schemes can improve system-level spectral efficiency, they are unable to achieve the capacity of the broadcast channel [1]. However, a non orthogonal multiple access (NOMA) scheme with superposition coding (SC) and successive interference cancellation (SIC) can achieve capacity in the Gaussian channel [2]. In [3], the optimal power, rate, and decoding order allocation for the superposition coding scheme are considered and shown that, at optimality, there is high probability that only two or three users are selected to be scheduled on one transmission channel. In spite of providing better system-level performance offered by NOMA, practical issues, such as user power allocation, signaling overhead, and SIC error propagation in its implementation are found [4]. The

authors of [5] show that the downlink NOMA with SIC improves cell edge user throughput performance and capacity. Furthermore, the NOMA/MIMO scheme using SIC and an interference rejection combining receiver is also proposed to meet the capacity gain requirement of future radio access. There are several NOMA techniques proposed in literature [6–9], including power domain NOMA (PD-NOMA), sparse code multiple access (SCMA) [6], pattern division multiple access (PDMA) [7], low density spreading (LDS) [8], and lattice partition multiple access (LPMA) [9]. All these techniques are based on the concept that more than one user is served in each orthogonal resource block. PD-NOMA has received greater research attention in this aspect because of its superior spectral efficiency realized by overloading with the ease of implementation [10]. PD-NOMA allows superposition-coded multi-user data to be concurrently transmitted by the same carrier. Here, users are differentiated in the power domain, and multi-user detection is accomplished by SIC. For high overloading factors, SIC requires increased hardware complexity and suffers from a processing delay at the receiver. Hence, it is best to multiplex not more than two users in a carrier [3,11]. Consequently, with single carrier NOMA (SC-NOMA), the overwhelming capacity demands of future generation networks cannot be met. However, these massive demands can be satisfied by a multi-carrier NOMA (MC-NOMA).

OFDM is a potential candidate for the realization of multi-carrier modulation in the 5G standard [12]. MC-NOMA realizes overloading with reduced complexity by integrating NOMA with existing multi-carrier frameworks like OFDMA [13]. This is accomplished by assigning each orthogonal subcarrier to two NOMA users. Optimal resource allocation and user pairing are crucial in order to fully reap the advantages of MC-NOMA. An OFDM-based NOMA system for the downlink, where signals corresponding to multiple users are transmitted on the same sub-band (time-frequency resource unit) using a superposition coding technique is presented in [1]. This work aims to maximize the weighted sum rate of the system by the optimal selection of the co-channel user set and power distribution among the users and sub-bands. Here, the availability of perfect channel state information at the base station is assumed. A similar resource allocation problem is studied in [14], which is a downlink OFDM-NOMA system. The resource allocation problem is treated as two sub-problems: subcarrier allocation (SA) and power allocation (PA). A novel OFDM-NOMA with a distinctive subcarrier spacing scheme is proposed to minimize the constraints associated with the multi-user detection operation [15]. Although this scheme ensures fairness among the users while improving the bit error rate performance, it is spectrally less efficient compared to the conventional equal subcarrier spacing of an OFDM-NOMA scheme. Downlink system-level performance of an OFDM-based NOMA, where a dynamic

multi-user power allocation scheme called fractional transmit power control (FTPC), similar to the transmission power control used in the LTE uplink, is studied in [16]. The authors in [17] have proposed a one-hop, non-cooperative half duplex MC-NOMA network with optimal joint power and subcarrier allocation for maximizing weighted system throughput. They have employed a similar optimization for a full duplex MC-NOMA network in [18]. However, cooperative communication, whose benefits are evident from several works in the literature [19,20], has not been considered in these two approaches.

Coordinated direct and relay transmission (CDRT) is a communication strategy that could further augment the network spectral efficiency by allowing multiple nodes to transmit simultaneously in a coordinated manner [21]. The CDRT network consists of a direct user and a relayed user. The direct user receives and decodes the relayed user data in the first hop of communication, that is, from source to relay. This knowledge is used to cancel out the interference in the second time slot when the direct user receives data from the source while the relay transmits to the relayed user. The CDRT used in [22] increases the achievable rate in a vehicular ad hoc network (VANET). CDRT requires side information for interference cancellation, and this side information is inherently available with NOMA [23]. Many works that explore the significance of CDRT are reported in literature [24–27]. It is proved in [24] that a NOMA-CDRT network achieves a better ergodic capacity than a non-CDRT network. The performance of an uplink two-user coordinated NOMA network is analyzed under perfect and imperfect SIC conditions in [25]. From this work, it is further evident that coordination can boost spectral efficiency and the performance gain obtained by a coordinated transmission depends on relay position and transmit signal-to-noise ratio (SNR). A novel NOMA-based dynamic CDRT scheme is proposed in [26], where the user close to the base station acts as a relay to the cell edge user in the second phase if it can obtain the prior information of the cell edge user in advance. Otherwise, it switches to the receiving mode. The selection of best-near and best-far users is done to improve the outage performance in a two-user NOMA-based cooperative relaying system, wherein simultaneous wireless information and power transfer is employed at the near user to power their relaying operations [27]. The cooperative relaying technique mandates two-hop communication, however, in a two-hop cooperative multi-carrier scenario, the optimal subcarrier pairing between the two hops is essential because a subcarrier that offers good channel gain in one hop may face deep fade in the next hop [28]. Therefore, to ensure good user throughput, subcarrier pairing is realized by using the Hungarian algorithm [29].

Cognitive radio (CR) is yet another key technology that addresses the spectrum scarcity problem by squeezing secondary users (SUs) into licensed bands [30]. A novel joint

spectrum sensing and access technique with interference cancellation for a CR network is proposed in [31]. Here, the cognitive user achieves greater throughput by a full duplex spectrum sensing technique, that is, one that simultaneously transmits its signal while sensing the spectrum. The resulting self-interference caused by the sensing process is cancelled using prior knowledge of the transmitted signal. As NOMA is also a special case of the underlay CR, it is reasonable to combine NOMA with CR to maximize spectrum utilization. The application of NOMA in underlay cooperative spectrum sharing is explored in [32] and the authors conclude that with the appropriate choice of target data rates and power allocation coefficients of users, NOMA can outperform OMA in underlay CR networks. A single carrier CR-NOMA network is presented in [33], and optimum power allocation coefficients are derived with the objective of maximizing the secondary system throughput. The outage probability of a NOMA transmission for a two-user underlay cognitive radio network (CRN) is studied in [34]. In all these works, the results apply only for a two-user network, and the system model in [34] is extended for multiple secondary users in [35]. In [36], a coordinated transmission scheme called analogue network coding (ANC) is used to increase the spectral efficiency in an underlay CR network consisting of a cognitive transmitter, a relay, and two cognitive receivers. It is shown that the use of coordinated transmission reduces the number of time slots required for communication from three to two. An overlay CR spectrum sharing scheme named CSS-NOMA-CDRT is proposed in [37]. This scheme exploits NOMA in both phases of coordinated direct and relay transmission. Another overlay cognitive spectrum sharing protocol using NOMA is proposed in [38] with space-time block coding that outperforms the conventional superposition coding-based protocol in terms of ergodic capacity and outage performance. However, multi-carrier transmission is not used in these studies. Authors in [39] have attempted the optimization of sensing duration and power allocation coefficients for a two-user underlay cognitive OFDM-NOMA network. However, this analysis is restricted to only two users and CDRT has not been considered.

A resource allocation problem in the cooperative cognitive relaying multi-carrier NOMA (MC-NOMA) system is presented in [40]. In this work, the secondary base station is used to exploit NOMA to serve multiple secondary users, and to simultaneously relay the information transmission to the primary network. A cooperative multi-user MC-NOMA network with CDRT is proposed in [41], and the throughput maximization problem is solved by optimizing power allocation, subcarrier assignment, relay selection, and subcarrier pairing. The non-convex optimization problem is solved using the Lagrange dual method. However, the solution algorithm suggested to optimize the power allocation

follows an exhaustive search approach and, thus, intensive computation. Further, CR-NOMA has not been considered in this work.

It is evident from the literature that research contributions to the integration of MC-NOMA in underlay cognitive networks with cooperative relaying is very limited and therefore this has become the focus of this work. In this work, an underlay cognitive network consisting of secondary users is squeezed into the system to maximize spectral utilization. The secondary users may receive information from a secondary base station (SBS), which also acts as a primary relay. Optimum power allocation is done for the underlay secondary user in each subcarrier with an interference constraint imposed by the primary users (PUs). For cognitive radio NOMA, the proper selection of a primary user target rate is important. The resulting overall network throughput is compared with the baseline scheme [41] and it is shown that the proposed network achieves a higher throughput. The main contributions of this work are as follows:

- An opportunistic underlay cognitive multi-carrier NOMA network is proposed.
- Joint optimization for resource allocation to the primary and secondary network has been achieved while satisfying the target rate constraints of primary network.
- A low complexity dynamic network resource allocation algorithm is proposed to solve the combinatorial optimization of near, far, and secondary user pairing, relay selection, and subcarrier pairing for throughput maximization.

The organization of this paper is as follows. Section 2 presents the model of the proposed opportunistic underlay multi-carrier cognitive NOMA network. In Section 3, the optimization problem is formulated and solved for throughput maximization of the proposed network. Simulation results that validate the proposed network throughput performance are provided and conclusions are drawn in Sections 4 and 5, respectively.

2 | NETWORK MODEL

The proposed downlink multi-carrier cooperative CR-NOMA network is illustrated in Figure 1. The system consists of a primary base station (PBS), multiple primary end users, and relays that can act as a secondary base station (SBS) for secondary users. The primary end users are categorized as near (direct) users (NU) or far (relayed) users (FU) based on their channel conditions with the PBS. The near users are located within the coverage area of the PBS and are capable of directly receiving messages from the PBS. In contrast, the far users are out of the coverage zone or have extremely weak links with the PBS; thus, they are
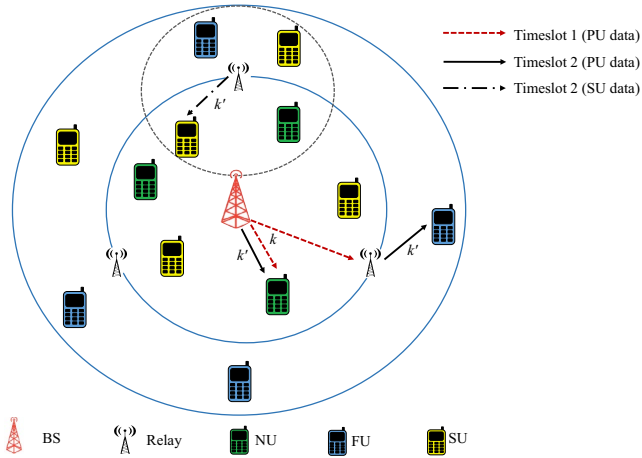
FIGURE 1 Network model

supported by relays located at the edge of near user zone. Information transfer from the PBS to primary users occurs in two time slots through relay in a coordinated direct mode and relay transmission mode. The relays are considered to follow the decode-and-forward scheme, where the information data received in the first time slot is forwarded with the same modulation rate to the second time slot. Therefore, the lengths of both time slots are considered to be equal. Based on the predefined priority conditions of the network, one of the relays will get an opportunity to serve the secondary users connected to it, and it is designated as a secondary base station. The SBS forwards the data to far users and, in addition, transmits the data to the secondary users connected to it in underlay mode. Primary user transmissions take place in both time slots whereas secondary users are opportunistically served only in the second time slot. OFDMA-based multi-carrier transmission is considered, and each orthogonal subcarrier is assumed to undergo flat fading over two time slots. A similar fading environment around PBS and relays has also been assumed. Likewise, it is assumed that perfect channel state information is available at the PBS as in [1,41] for users and relays.

It is assumed that the network consists of N near users, F far users, C cognitive users, L relays and K orthogonal subcarriers. Let $N = \{1, 2, \ldots, N\}$, $F = \{1, 2, \ldots, F\}$, $C = \{1, 2, \ldots, C\}$, $L = \{1, 2, \ldots, L\}$, and $K = \{1, 2, \ldots, K\}$ denote the set of near users, far users, secondary (cognitive) users, relays, and subcarriers respectively. All the subcarriers in set K are utilized in both time slots. Each subcarrier in time slot 1 (direct transmission), $k \in K$, is paired with a subcarrier $k' \in K$ in time slot 2 (coordinated transmission). Let $\ell^* \in L$ denote the relay that serves secondary users opportunistically and $\ell \in L \setminus \ell^*$ denote any relay other than ℓ^*. Relaying data to FUs takes place in time slot 2 and one or more relays take part in relaying messages based on channel conditions. It should be noted that collectively all subcarriers are utilized by the participating relays and base station. The PBS fully utilizes

the subcarriers to transmit the data to near users and relays in first time slot, and transmits data only to near users in second time slot. In the second time slot, the subcarriers are shared by relays for the relaying of FU's data. In the same time slot, the unused subcarriers at relay ℓ^* (SBS) are used to serve underlay secondary users. However, the unused subcarriers in ℓ^* are simultaneously being used by PBS to serve other NU-FU pairs and another relay $\ell \in L \setminus \ell^*$.

In this present work, considering primary and secondary channel conditions, optimum power allocation has been carried out for PBS, SBS, and relays while satisfying primary user target rate constraints on throughputs of NUs and FUs. During this process, the power allocation for subcarriers assigned to underlay SU transmission in SBS has also been determined. The transmission mechanism and signal model are developed in the following subsections.

2.1 | Notation

The variables $x_{i,j}$, $y_{i,j}$, and $z_{i,j}$ denote a message transmitted in subcarrier i to NU j, FU j, and SU j, respectively. $w_j^{(i)}$ denotes the complex additive white Gaussian noise (AWGN) with $\mathcal{N}(0, \sigma^2)$ in time slot i at node j. $h_{i,j}^S$ is the channel coefficient from station S to j in subcarrier i, which is a function of distance and Rayleigh fading. $g_{i,j}^S = (|h_{i,j}^S|^2)/\sigma^2$ is the channel-to-noise ratio (CNR) from S to j in subcarrier i. $p_{i,j}^S$ represents the power allocated at station S to the signal intended for node j in subcarrier i.

2.2 | Time slot 1: Direct transmission

The subcarrier k in the first time slot is paired with k' in the second time slot for the near-user n, far-user f pair and relay l of the primary system. In the first time slot, the PBS transmits a message intended for a NU and a FU using PD-NOMA. This transmission is received by the NU n and the relay l selected for FU f, but not by FU f, because they are out of the coverage zone. The relays decode the corresponding FU's messages to forward them in the second time slot. The superposition coded signal transmitted by the PBS in subcarrier k to NU n and FU f in the first time slot is given by $\sqrt{p_{k,n}^{BS,1}} x_{k,n} + \sqrt{p_{k,f}^{BS,1}} y_{k,f}$, where $x_{k,n}$ and $y_{k,f}$ are the messages intended for NU n and FU f, respectively, in subcarrier k, and $p_{k,n}^{BS,1}$ and $p_{k,f}^{BS,1}$ denote the corresponding transmit powers. In time slot 1, the received signals at NU n and relay l, respectively, in subcarrier k are

$$r_{k,n}^{(1)} = \left(\sqrt{p_{k,n}^{BS,1}} x_{k,n} + \sqrt{p_{k,f}^{BS,1}} y_{k,f} \right) h_{k,n}^{BS} + w_n^{(1)}, \quad (1)$$

$$r_{k,l}^{(1)} = \left(\sqrt{p_{k,n}^{BS,1}} x_{k,n} + \sqrt{p_{k,f}^{BS,1}} y_{k,f} \right) h_{k,l}^{BS} + w_l^{(1)}. \quad (2)$$

Because relays are located at the edge of the near-user zone, based on channel conditions the channel gains are ordered as $|h_{k,n}^{BS}|^2 > |h_{k,l}^{BS}|^2$.

The far user is allocated more power, and hence, the relay l directly decodes the data pertaining to FU f, considering the near user message as interference. In contrast, the NU n must perform SIC first to estimate and cancel out the message intended for FU f from $r_{k,n}^{(1)}$ before decoding its own message. The SNR at NU n and signal-to-interference-plus-noise ratio (SINR) at relay l in subcarrier k, for decoding $x_{k,n}$ and $y_{k,f}$, respectively, are

$$\rho_{k,n}^{(1)} = p_{k,n}^{BS,1} g_{k,n}^{BS}, \tag{3}$$

$$\rho_{k,l,f}^{(1)} = \frac{p_{k,f}^{BS,1} g_{k,l}^{BS}}{p_{k,n}^{BS,1} g_{k,l}^{BS} + 1}. \tag{4}$$

The achievable rates at NU n and relay l, respectively, in subcarrier k, in the first time slot are given by

$$R_{k,n}^{(1)} = \frac{1}{2} \log_2 (1 + \rho_{k,n}^{(1)}), \tag{5}$$

$$R_{k,l,f}^{(1)} = \frac{1}{2} \log_2 (1 + \rho_{k,l,f}^{(1)}). \tag{6}$$

2.3 | Time slot 2: Coordinated transmission

In the coordinated transmission slot, a new message, $x'_{k',n}$, is transmitted to NU n by PBS using k'. The subcarrier k' may be different from k. The signal transmitted by PBS to NU n in k' is $\sqrt{p_{k',n}^{BS,2}} x'_{k',n}$. Concurrently, $y_{k,f}$ is relayed to FU f by a selected relay l in subcarrier k', and is denoted here as $y_{k',f}$.

The selected relay l could belong to any one of two possible categories:

- $l = \ell^*$, SBS, which opportunistically serves SUs.
- $l = \ell \in L \backslash \ell^*$, relays other than SBS, which serve PUs only.

If k' is allotted to relay $l = \ell^*$, the signal transmitted to FU f in k' is given by $\sqrt{p_{k',f}^{\ell^*}} y_{k',f}$. As k' is paired to ℓ^*, it is not used for transmitting SU's messages. Received signals at NU n and FU f, respectively, in k' are given by

$$r_{k',n}^{(2)} = \sqrt{p_{k',n}^{BS,2}} x'_{k',n} h_{k',n}^{BS} + \sqrt{p_{k',f}^{\ell^*}} y_{k',f} h_{k',n}^{\ell^*} + w_n^{(2)}, \tag{7a}$$

$$r_{k',f}^{(2)} = \sqrt{p_{k',f}^{\ell^*}} y_{k',f} h_{k',f}^{\ell^*} + w_f^{(2)}. \tag{7b}$$

In (7a), the second term is the interference from the FU transmission on the NU, which takes place in the same subcarrier. However, this term can be removed by the NU with the knowledge of $y_{k',f}$ obtained from the previous slot. Additionally, in (7b), the interference at the FU from PBS transmissions has been omitted because it is negligible due to its extremely weak link with PBS.

In contrast, if k' is not allotted to SBS for the transmission of the primary user's message, it is used by SBS for transmitting the message to secondary user c, $(c \in C)$ in underlay mode. The signal transmitted in k' by relays ℓ and ℓ^*, respectively, are $\sqrt{p_{k',f}^{\ell}} y_{k',f}$ and $\sqrt{p_{k',c}^{\ell^*}} z_{k',c}$. Now, the received signal at NU n and FU f, respectively, in k' will be

$$r_{k',n}^{(2)} = \sqrt{p_{k',n}^{BS,2}} x'_{k',n} h_{k',n}^{BS} + \sqrt{p_{k',f}^{\ell}} y_{k',f} h_{k',n}^{\ell} + \sqrt{p_{k',c}^{\ell^*}} z_{k',c} h_{k',n}^{\ell^*} + w_n^{(2)}, \tag{8a}$$

$$r_{k',f}^{(2)} = \sqrt{p_{k',f}^{\ell}} y_{k',f} h_{k',f}^{\ell} + \sqrt{p_{k',c}^{\ell^*}} z_{k',c} h_{k',f}^{\ell^*} + w_f^{(2)}. \tag{8b}$$

Similar to the case in (7a), the second term in (8a) can be removed at the NU because it has prior knowledge of it. The third term in (8a) is the interference from the underlay transmission by ℓ^*. Also, the interference from PBS transmissions is negligible at FU, and that from underlay transmissions is given by the second term of (8b). From (7) and (8), the SINR in time slot 2 at NU n and FU f, respectively, in k' are given by

$$\rho_{k',n}^{(2)} = \begin{cases} p_{k',n}^{BS,2} g_{k',n}^{BS} & \text{if } l = \ell^*, \\ \frac{p_{k',n}^{BS,2} g_{k',n}^{BS}}{p_{k',c}^{\ell^*} g_{k',n}^{\ell^*} + 1} & \text{if } l \neq \ell^*, \end{cases} \tag{9}$$

$$\rho_{k',f}^{(2)} = \begin{cases} p_{k',f}^{\ell^*} g_{k',f}^{\ell^*} & \text{if } l = \ell^*, \\ \frac{p_{k',f}^{\ell} g_{k',f}^{\ell}}{p_{k',c}^{\ell^*} g_{k',f}^{\ell^*} + 1} & \text{if } l \neq \ell^*. \end{cases} \tag{10}$$

In the subcarriers allotted to $l = \ell^*$, the interference to the SUs from PUs is zero and the SINR becomes SNR.

It is assumed that SUs are located randomly as a cluster around ℓ^* and it is possible that they lie within or out of PBS coverage. If the relay selected to forward far user data in subcarrier k' is the SBS, that is, if $l = \ell^*$, then no transmission to the secondary takes place in k' (that is, $z_{k',c} = 0$) because ℓ^* has to serve the primary user in k'. In contrast, if the relay selected to forward far user information in k' is not ℓ^*, that is, if $l = \ell$, then ℓ^* is free to transmit to a secondary user using k'. When $l = \ell \in L \backslash \ell^*$, the received signal at SU c in subcarrier k', if it lies within PBS coverage, is

$$r_{k',c}^{(2)} = \sqrt{p_{k',c}^{\ell^*}} z_{k',c} h_{k',c}^{\ell^*} + \sqrt{p_{k',n}^{BS,2}} x'_{k',n} h_{k',c}^{BS} + \sqrt{p_{k',f}^{\ell}} y_{k',f} h_{k',c}^{\ell} + w_c^{(2)}. \tag{11}$$

If SU c lies out of PBS coverage, it will not receive PBS transmissions and the second term of (11) will be zero. The SINR at SU c in k' is

$$\rho_{k',c}^{(2)} = \begin{cases} 0 & \text{if } l = \ell^*, \\ \dfrac{p_{k',c}^{\ell^*} g_{k',c}^{\ell^*}}{p_{k',n}^{BS,2} g_{k',n}^{BS} + p_{k',f}^{l} g_{k',f}^{l} + 1} & \text{if } l \neq \ell^*. \end{cases} \quad (12)$$

The primary transmissions in k' are present as interference in the denominator of (12) when $l \neq \ell^*$.

Achievable rates at NU n, FU f and SU c in subcarrier k' at time slot 2 are, respectively,

$$R_{k',n}^{(2)} = \frac{1}{2} \log_2 \left(1 + \rho_{k',n}^{(2)}\right), \quad (13)$$

$$R_{k',f}^{(2)} = \frac{1}{2} \log_2 \left(1 + \rho_{k',f}^{(2)}\right), \quad (14)$$

$$R_{k',c}^{(2)} = \frac{1}{2} \log_2 \left(1 + \rho_{k',c}^{(2)}\right). \quad (15)$$

At the end of the two time slots, the weighted achievable sum rate of the system in subcarrier pair (k, k') is given by

$$\begin{aligned} R_{n,f,l,c}^{k,k'} = {}& \omega_n R_{k,n}^{(1)} + \omega_n R_{k',n}^{(2)} \\ & + \omega_f \min\left(R_{k,l,f}^{(1)}, R_{k',f}^{(2)}\right) + \omega_c R_{k',c}^{(2)}. \end{aligned} \quad (16)$$

The weighted sum rate is considered to incorporate user fairness [42]. In (17), ω_n, ω_f, and ω_c denote the weight factors of NU n, FU f and SU c respectively. Weight factors are provided to PUs (NUs and FUs) based on their distance from the PBS in such a way that the farthest user is given the maximum weight value. In this work, it is assumed that the location and distance of the end users are known by using mobile positioning techniques described in several works in the literature [43,44]. For the primary system, the weight factors are $\omega_a = d_a / \left(\sum_{j=1}^{N+F} d_j\right)$, where $a = 1, 2, \dots, N+F$. For the secondary system, the weight factors are assigned as $\omega_b = d_b / \left(\sum_{j=1}^{C} d_b\right)$, where $b = 1, 2, \dots, C$. d_a and d_b are the distances of ath PU and b^{th} SU from the PBS and SBS, respectively.

The first three terms of (16) relate to primary user throughput (T_p) and the last term relates to secondary user throughput (T_s).

It should be noted that, in the network, all relays collectively utilize all subcarriers to serve FUs. At any given relay, only a subset of subcarriers is utilized, and no two relays are assigned to transmit with the same subcarrier to the FUs. The following notations are used in the next section. κ_i denotes a set of subcarriers assigned to relay i, $(i = 1, 2, \dots, L)$ to serve the FUs associated with it. Then, $\kappa_1 \cup \kappa_2 \cup \cdots \kappa_L = \mathbf{K}$ and $\kappa_i \cap \kappa_j = \emptyset, (i \neq j)$. In the proposed scheme, one of the relays, $l = \ell^*$, is also designated as the SBS to opportunistically serve underlay SUs with its unused subcarriers $\{\mathbf{K} - \kappa_{\ell^*}\}$. R^* denotes the target rate of the NUs and FUs in each subcarrier. In the following section, the optimization problem for network throughput maximization is formulated and solved.

3 | NETWORK THROUGHPUT MAXIMIZATION

3.1 | Problem formulation

Considering the combinations of near and far primary users, relays, secondary users, and subcarrier pairs, the total achievable network throughput is given by

$$T = \sum_{k=1}^{K} \sum_{k'=1}^{K} \sum_{n=1}^{N} \sum_{f=1}^{F} \sum_{l=1}^{L} \sum_{c=1}^{C} \xi_{n,f,l,c}^{k,k'} R_{n,f,l,c}^{k,k'}, \quad (17)$$

where $\xi_{n,f,l,c}^{k,k'} \in \{0,1\}$ and $\xi_{n,f,l,c}^{k,k'} = 1$ if subcarrier k in the first slot is paired with k' in the second slot and this pair is assigned to NU n, FU f, relay l and SU c. Otherwise, $\xi_{n,f,l,c}^{k,k'} = 0$.

The joint optimization problem of network throughput maximization is formulated as follows:

$$\textbf{OP1} \quad \max_{\xi_{n,f,l,c}^{k,k'}, p_{k,n}^{BS,1}, p_{k,f}^{BS,1}, p_{k',n}^{BS,2}, p_{k',f}^{l}, p_{k',c}^{\ell^*}} T$$

subject to

$$\sum_{k=1}^{K} \left(\sum_{n=1}^{N} p_{k,n}^{BS,1} + \sum_{f=1}^{F} p_{k,f}^{BS,1}\right) \leq P_{\max}^{BS}, \quad (C1)$$

$$\sum_{k'=1}^{K} \sum_{n=1}^{N} p_{k',n}^{BS,2} \leq P_{\max}^{BS}, \quad (C2)$$

$$\sum_{k'=1}^{K} \sum_{f=1}^{F} p_{k',f}^{l} \leq P_{\max}^{l} \quad \forall l, \text{except } l = \ell^*, \quad (C3)$$

$$\sum_{k'=1}^{K} \left(\sum_{f=1}^{F} p_{k',f}^{\ell^*} + \sum_{c=1}^{C} p_{k',c}^{\ell^*}\right) \leq P_{\max}^{\ell^*}, \quad (C4)$$

$$\rho_{k,l,f}^{(1)} = \rho_{k',f}^{(2)} \quad \forall(k, k', f, l), \quad (C5)$$

$$\sum_{l=1}^{L}\sum_{n=1}^{N}\sum_{f=1}^{F}\sum_{c=1}^{C}\xi_{n,f,l,c}^{k,k'}\leq 1 \quad \forall(k,k'), \tag{C6}$$

$$\sum_{k=1}^{K}\xi_{n,f,l,c}^{k,k'}\leq 1 \quad \forall(k',n,f,l,c), \tag{C7}$$

$$\sum_{k'=1}^{K}\xi_{n,f,l,c}^{k,k'}\leq 1 \quad \forall(k,n,f,l,c), \tag{C8}$$

$$\xi_{n,f,l,c}^{k,k'}\in\{0,1\} \quad \forall(k,k',n,f,l,c), \tag{C9}$$

$$R_{k',n}^{(2)}\geq R^* \quad \forall k'\in\{K-\kappa_{\ell*}\},n, \tag{C10}$$

$$R_{k',f}^{(2)}\geq R^* \quad \forall k'\in\{K-\kappa_{\ell*}\},n. \tag{C11}$$

The constraints (C1) to (C4) ensure that the maximum transmit power is not exceeded at the PBS (P_{max}^{BS}) and relays (P_{max}^{l}, $P_{max}^{\ell*}$). Because the achievable rate of the FU is dominated by the SINR of the weakest link in the two hop communication, the transmit power level of the hop with high SINR is reduced so as to make the SINRs of both hops equal (as in [41]). This leads to the constraint (C5). The constraint (C6) guarantees that a given subcarrier pair is exclusively assigned to only one NU, FU, relay, and SU. (C7) and (C8) ensure one-to-one subcarrier pairing. The variable $\xi_{n,f,l,c}^{k,k'}$ can take only binary values as given by (C9). (C10) and (C11) guarantee that the NU and FU target rate (R^*) are met in each subcarrier, despite interference from SU transmissions. It should be noted that a FU can receive different messages from more than one relay on different subcarriers.

3.2 | Solution to optimization problem

The solution to OP1 optimizes the following parameters: $p_{k,n}^{BS,1}$, $p_{k,f}^{BS,1}$, $p_{k',n}^{BS,2}$, $p_{k',f}^{l}$, $p_{k',c}^{\ell*}$, and $\xi_{n,f,l,c}^{k,k'}$. In an underlay cognitive radio scenario, priority is given to the PUs, which are oblivious to the presence of SUs. However, SUs are aware of the PU transmission levels and adjust their own transmission power accordingly so that they do not create a considerable amount of interference to the PUs. Therefore, by giving priority to PUs, the initial values of $p_{k,n}^{BS,1}$, $p_{k,f}^{BS,1}$, $p_{k',n}^{BS,2}$, and $p_{k',f}^{l}$ are calculated as a first step by setting $p_{k',f}^{\ell*}=0$. Once the initial power levels of primary users are calculated, the SBS calculates the acceptable power levels for SUs ($P_{k',c}^{\ell*}$). In the next step, to choose the optimum combinations of (k,k',n,f,l,c) that satisfy constraints (C6)–(C9)

and also maximize throughput, combinatorial optimization is carried out. That is, the optimization of $\xi_{n,f,l,c}^{k,k'}$. In the final step, the power levels are optimized by using the ellipsoidal algorithm.

Because OP1 is non-convex, a dual optimization problem is formulated based on the Lagrange method [45]. The dual problem of OP1 is formulated as

$$\mathbf{OP2} \min_{\lambda,\mu,\nu} g(\lambda,\mu,\nu),$$

subject to

$$\lambda,\mu,\nu\geq 0.$$

The expression for $g(\lambda,\mu,\nu)$ and the optimum $p_{k,n}^{BS,1}$, $p_{k,f}^{BS,1}$, $p_{k',n}^{BS,2}$, and $p_{k',f}^{l}$ can be found in (14), (17), and (18) of [41]. Giving priority to the primary users, powers of PU transmissions have been identified by solving OP2 as explained in [41]. Followed by the power allocations for PUs, the SBS calculates the secondary power allocation satisfying (C10) and (C11) as follows:

The power allocation for the secondary user c in the SBS $p_{k',c}^{\ell*}$ is calculated by equating the achievable rate at the NU n and FU f in subcarrier k' to their target rate R^* that is, $R_{k',n}^{(2)}=R_{k',f}^{(2)}=R^*$.

$$R_{k',n}^{(2)}=\frac{1}{2}\log_2\left(1+\frac{p_{k',n}^{BS,2}g_{k',n}^{BS}}{p_{k',c}^{\ell*}g_{k',n}^{\ell*}+1}\right)=R^*, \tag{18}$$

$$R_{k',f}^{(2)}=\frac{1}{2}\log_2\left(1+\frac{p_{k',f}^{l}g_{k',f}^{l}}{p_{k',c}^{\ell*}g_{k',f}^{\ell*}+1}\right)=R^*. \tag{19}$$

By solving (18) and (19) for $p_{k',c}^{\ell*}$, the following is obtained:

$$p_{1,k',c}^{\ell*}=\max\left\{0,\left(\frac{p_{k',n}^{BS,2}g_{k',n}^{BS}}{\varepsilon}-1\right)\frac{1}{g_{k',n}^{\ell*}}\right\}, \tag{20a}$$

$$p_{2,k',c}^{\ell*}=\max\left\{0,\left(\frac{p_{k',f}^{l}g_{k',f}^{BS}}{\varepsilon}-1\right)\frac{1}{g_{k',f}^{\ell*}}\right\}, \tag{20b}$$

$$p_{k',c}^{\ell*}=\min\left(p_{1,k',c}^{\ell*},p_{2,k',c}^{\ell*}\right), \tag{20c}$$

where $\varepsilon=2^{2R^*}-1$ is the target SINR of the primary users. Equation (20c) ensures that the power allocated to secondary users does not affect the target rates of NU and FU pertaining to the carrier k'. Then, the combinatorial optimization is applied to the calculation of $\xi_{n,f,l,c}^{k,k'}$.

Following the exhaustive search-based optimization procedure used in [41], which requires K^2NFLC computations for optimizing $\xi_{n,f,l,c}^{k,k'}$ and the power allocations $p_{k,n}^{BS,1}, p_{k,f}^{BS,1}, p_{k',n}^{BS,2}, p_{k',f}^{l}$, and $p_{k',c}^{\ell^*}$. To reduce computational complexity, a dynamic network resource allocation algorithm has been proposed for the combinatorial optimization as summarized in Algorithm 1.

3.2.1 | Computation complexity of proposed algorithm

The number of computations involved in the calculation of the power level of PBS and relays for each subcarrier in the proposed algorithm is calculated as follows. Step 2 of the algorithm requires $NFLC$ computations because power levels are calculated for only one subcarrier pair. Step 4 requires K^2 computations because, for a given (n, f, l, c) combination, power levels are calculated for all possible subcarrier pairings. Because K optimum subcarrier pairs are obtained as the output of the Hungarian algorithm (step 5), and each subcarrier pair requires $NFLC$ computations, a total of $KNFLC$ computations are required in step 6.

Overall, the total number of computations required by the proposed dynamic apporach is equal to $NFLC(1 + K) + K^2$. The exhaustive approach requires K^2NFLC computations. A comparison of the number of computations required in both the approaches is presented in Table 1. It can be seen that for $K = 72, N = 16, F = 24, L = 3$, and $C = 72$, the exhaustive approach requires approximately 430 million computations. For the same numbers, the proposed dynamic method requires approximately only 6 million computations. Thus, the overall computational complexity is significantly reduced. As a result, the energy resources needed for computation can be conserved and computation time can also be reduced by approximately 70 times.

The calculated primary and secondary power levels and $\xi_{n,f,l,c}^{k,k'}$ are applied to the ellipsoid algorithm [46] to minimize $g(\lambda,\mu,\nu)$. In this proposed work, the subgradients to update the ellipsoid in the ith iteration are

$$\Delta\lambda(i) = P_{max}^{BS} - \sum_{k=1}^{K}\left(\sum_{n=1}^{N}p_{k,n}^{BS,1} + \sum_{f=1}^{F}p_{k,f}^{BS,1}\right), \quad (21a)$$

$$\Delta\mu(i) = P_{max}^{BS} - \sum_{k'=1}^{K}\sum_{n=1}^{N}p_{k',n}^{BS,2}, \quad (21b)$$

$$\Delta\nu_l(i) = P_{max}^{l} - \sum_{k'=1}^{K}\sum_{f=1}^{F}p_{k',f}^{l}, \quad \forall l \in L\backslash\ell^*, \quad (21c)$$

TABLE 1 Number of computations in exhaustive search and proposed methods

					Number of computations	
N	F	L	K	C	Exhaustive search	Proposed
2	2	3	4	4	768	256
4	4	3	12	12	82 944	7632
8	8	3	16	16	786 432	52 480
16	24	3	72	72	429 981 696	6 060 096

$$\Delta\nu_{\ell^*}(i) = P_{max}^{\ell^*} - \sum_{k'=1}^{K}\left(\sum_{f=1}^{F}p_{k',f}^{\ell^*} + \sum_{c=1}^{C}p_{k',c}^{\ell^*}\right) \quad \forall l = \ell^*. \quad (21d)$$

Equation (21d) ensures that the constraint on the maximum transmit power used by the SBS has not been violated by the introduction of secondary users in the network.

4 | RESULTS

The simulated throughput performance of the proposed system is presented in this section. In the simulated scenario, near users are randomly located following a uniform distribution within a circular disc of radius 500 m, with the PBS located at the center. Far users are uniformly located in the annular region between 500 m and 800 m from the PBS, and the three relays are uniformly placed at the inner disc boundary. There are several secondary users available in the coverage region of the relays. The SUs are connected to a relay with which they have good channel conditions. It may be noted that the SUs that are connected to a relay designated as SBS alone will be served. The multi-carrier system, which is realized in the form of an OFDMA, allows each subcarrier to undergo zero mean, unit variance Rayleigh flat fading. Path loss is considered to be $128 + 37.6\log_{10}(d)$, as in [47], where d is the distance between the transmit and receive nodes, in km. A shadowing of 10 dB is considered, and the subcarrier spacing is assumed to be 15 kHz. Furthermore, the maximum transmit power at each relay is lower than the maximum PBS transmit power (P_{max}^{BS}) by 13 dB. The throughput performances were studied by varying primary user target rate, maximum transmit powers of PBS, number of subcarriers, and number primary users. These simulation parameters have been summarized in Table 2.

For the different target rate requirements of a primary user, throughput performance of the proposed system has been studied along with a baseline system in [41], which consists of only primary users and no underlay cognitive users. The network is simulated with 16 near users, 24 far users, 72 secondary users, 3 relays, and 72 subcarriers. The

Algorithm 1 Dynamic network resource allocation algorithm

1. **Input:** Initialize weight factors $(\omega_n, \omega_f, \omega_c)$, maximum transmit powers of PBS and relay $(P_{max}^{BS}, P_{max}^l)$ and initial Lagrange multipliers (λ, μ, ν)

2. Select an arbitrary (k, k'), and calculate $p_{k,n}^{BS,1}, p_{k,f}^{BS,1}, p_{k',n}^{BS,2}, p_{k',f}^l$, and $p_{k',c}^{\ell*}$ for all possible combinations of (n, f, l, c)

3. Choose (n, f, l, c) combination that offers maximum throughput for the selected (k, k') pair

4. For the chosen (n, f, l, c), compute optimum power allocation and resulting throughput for all K^2 possible subcarrier pair combinations

5. Apply the Hungarian algorithm [29] and get the optimum subcarrier pairing for the chosen (n, f, l, c)

6. For each optimum subcarrier pair, do optimum power allocation and calculate the resulting throughput for all possible (n, f, l, c) combinations. Choose (n, f, l, c) that offers maximum throughput

7. Calculate sub-gradients and update the ellipsoid using (21).

8. **if** the ellipsoid stop criterion is not satisfied, go to step 2

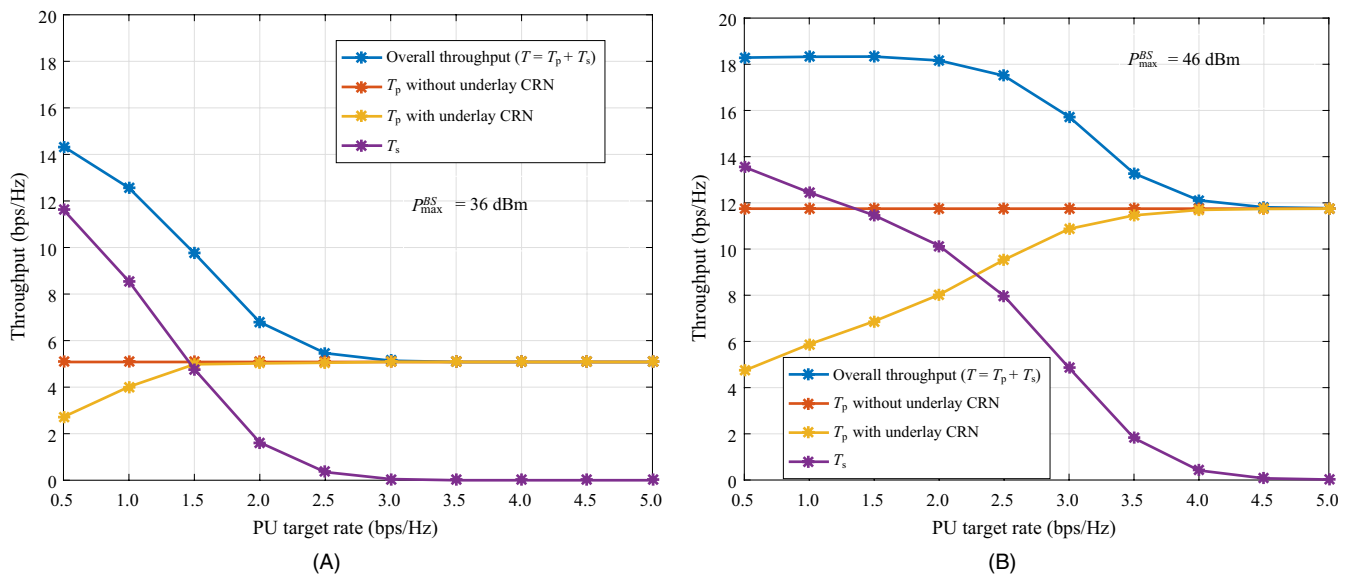9. **Output:** Optimum resource allocation solutions

TABLE 2 Simulation parameters

Max. PBS transmit power P_{max}^{BS}	36 dBm−46 dBm
Max. relay transmit power P_{max}^l	$P_{max}^{BS} - 13$ dB
PU target rate per subcarrier	0.5 bps/Hz to 5 bps/Hz
Number of NUs (N)	16–32
Number of FUs (M)	24−40
Number of SUs (C)	10−100
Number of subcarriers (K)	36−104
Number of relays (L)	3
Subcarrier spacing	15 kHz
Path loss	$128 + 37.6 \log_{10}(d)$
Shadowing	10 dB

transmission powers of 36 dBm and 46 dBm, respectively. In the presence of SUs, the overall system throughput has been improved due to the opportunity provided for SUs. For low primary user target rates, the overall network throughput improvement is significant because the SUs get more opportunities to be served. The PUs get a reduction in throughput but with an ensured target rate. However, as the target rate increases, the opportunistic secondary transmission becomes weaker because the secondary transmit power is reduced to minimize the interference to the primary users. Thus, for high PU target rates, SU throughput approaches zero, and the overall system throughput approaches the baseline system throughput because the secondary network is not served at all. It is observed from Figure 2 that the throughput of the SUs approaches zero beyond the target rate of 3 bps/Hz and 4.5 bps/Hz for 36 dBm and 46 dBm of PBS transmit powers, respectively. Furthermore, it can be observed that for a smaller reduction

throughputs offered by primary users (T_p), secondary users (T_s), and overall system T, have been obtained by varying primary user target rate from 0.5 bps/Hz to 5 bps/Hz [48,49] for PBS transmit powers of 36 dBm and 46 dBm, respectively, shown in Figure 2A and 2B, respectively.

It is observed from Figure 2A and 2B that the baseline system offers a uniform throughput of 5 bps/Hz and 12 bps/Hz irrespective of primary user target rates for the PBS

FIGURE 2 Network throughput vs PU target rate for different transmit powers: (A) $P_{max}^{BS} = 36$ dBm and (B) $P_{max}^{BS} = 46$ dBm

in the throughput of the primary network compared to baseline system, there is a greater improvement in overall system throughput. For example, despite a reduction of 40% in primary throughput, at a PBS power of 36 dBm, the overall network throughput improves by 180\% at a target rate of 0.5 bps/Hz.

The system throughput as a function of PBS transmit power has been studied in Figure 3 for primary user target rates of {2.0, 2.5, 3.0, 3.5} bps/Hz. It is observed that the overall system throughput increases with an increase in transmission power. Furthermore, it is observed that the minimum PBS transmit power at which the opportunistic secondary transmission can occur increases as the target rate increases. For an example, the SUs get an opportunity with significant throughput for a PBS transmission power of 36 dBm at a target rate of 2 bps/Hz, but the opportunity starts only above 42 dBm at a target rate of 3.5 bps/Hz.

From the above results, it is evident that the primary target rate of 3 bps/Hz and transmission power of 46 dBm offers an insignificant loss in primary user throughput and significant improvement in overall system throughput. The study on the impact of number of subcarriers, and number of near, far, and secondary users in throughput performance have been carried out with these values.

Network throughput has been obtained in Figure 4A as a function of the number of subcarriers for the presence of 16 NUs, 24 FUs, and 72 SUs. It is observed from the curves that the achievable primary and secondary system throughput improves as the number of subcarriers increases, thereby the overall system throughput also increases. The improvement in overall system throughput becomes more significant for a higher number of subcarriers. There is a smaller reduction in the primary user achievable rate compared to baseline system, and it is uniform.
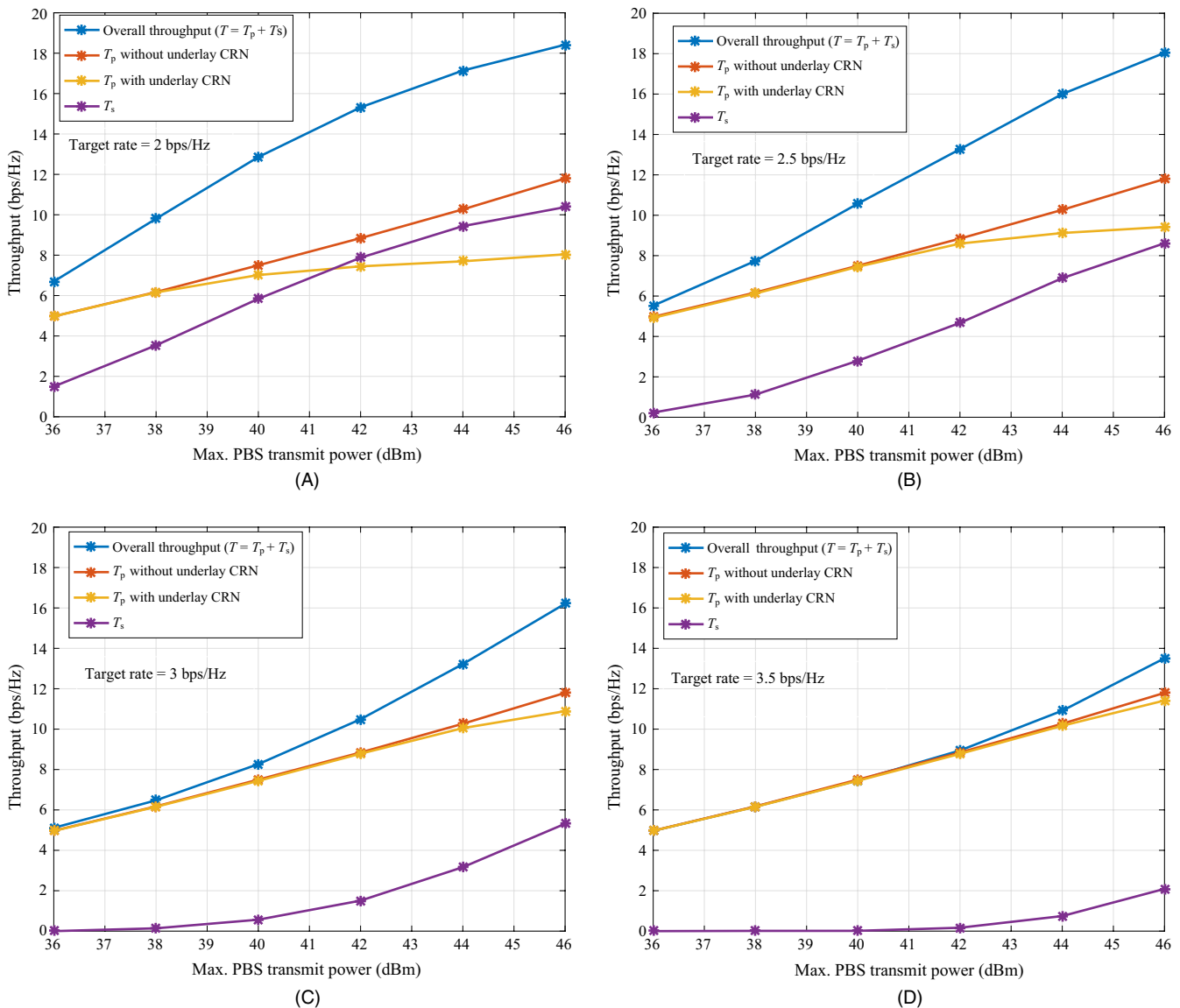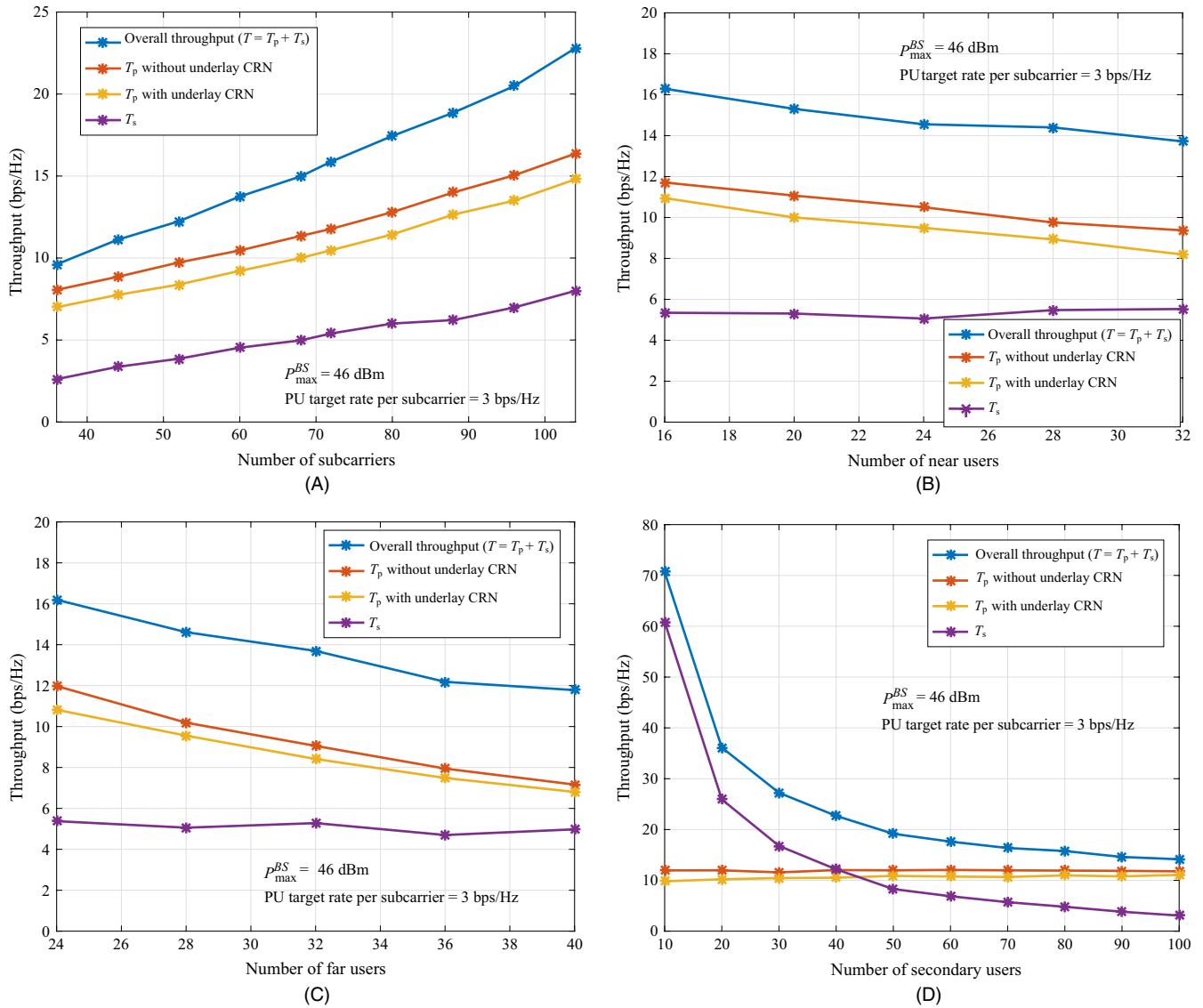

FIGURE 3 Network throughput vs transmit power for different PU target rates: (A) 2 bps/Hz, (B) 2.5 bps/Hz, (C) 3 bps/Hz, and (D) 3.5 bps/Hz

FIGURE 4 Network throughput for different numbers of (A) subcarriers, (B) near users, (C) far users, and (D) secondary users, at $P_{max}^{BS} = 46$ dBm and PU target rate per subcarrier = 3 bps/Hz

The network throughput for a different number of near, far, and secondary users have been obtained as shown in Figure 4B to 4D, respectively, by selecting 72 subcarriers and keeping all other parameters the same as used above. As the number of near/far/secondary users is increased, a reduction in system throughput is observed. This is due to the fact that the demand for a fair subcarrier pair increases with an increased number of users. This also reduces the opportunity for secondary users and, hence, the throughput.

Comparing Figure 4B with 4C, the reduction in system throughput is higher as the number of far users increases. This is because the throughput function is maximized with a higher weight factor given to the far users. From Figure 4D, it is observed that the improvement in overall system throughput is very large for smaller number of secondary users because

they acquire more opportunity. While the number of secondary users increases, the overall system throughput exponentially decreases and approaches the throughput of the baseline system. This is because the optimization has been done with a higher weight factor allocated for weak users and, hence, the rate offered by secondary users becomes smaller as secondary users increases. It has been observed from the results discussed above that the presence of underlay CR secondary users will improve the overall throughput of a multi-carrier NOMA network.

5 | CONCLUSION

A throughput maximization problem with joint resource allocation in a multi-carrier NOMA network supporting underlay CR users is formulated and solved. The dynamic resource

allocation algorithm for combinatorial optimization proposed in this work reduces the computational complexity by a factor approximately equal to K (number of subcarriers), as compared to exhaustive search algorithms. For 72 subcarriers, it was found that the number of computations is reduced from approximately 430 million to 6 million, which is approximately a reduction by 70 times. By adding an underlay CRN to a multi-carrier NOMA network, the overall system throughput is significantly increased at the cost of a smaller reduction in achievable throughput of PUs without compromising primary target rate. The numerical results obtained from simulations confirmed the significance of the proposed algorithm.

ORCID

Sparjan Romera Joan (iD) https://orcid.org/0000-0002-9767-0822

REFERENCES

1. P. Parida and S. S. Das. *Power allocation in OFDM based NOMA systems: A DC programming approach*, in Proc. IEEE Globecom Workshops (Austin, TX, USA), 2014, pp. 1026–1031.
2. D. Tse and P. Viswanath, Fundamentals of Wireless Communications (1st ed), Cambridge University Press, Cambridge, UK, 2004.
3. A. Zafar et al. *On multiple users scheduling using superposition coding over rayleigh fading channels*, IEEE Commun. Lett. **17** (2013), no. 4, 733–736.
4. A. Benjebbour et al., *Concept and practical considerations of non-orthogonal multiple access (NOMA) for future radio access*, in Proc. Int. Symp. Intell. Signal Process. Commun. Syst. (Okinawa, Japan), 2013, pp. 770–774.
5. Y. Saito et al., *Non-orthogonal multiple access (NOMA) for cellular future radio access*, in Proc. IEEE 77th Veh. Technol. Conf. (Dresden, Germany), 2013, pp. 1–5.
6. H. Nikopour and H. Baligh, *Sparse code multiple access*, in Proc. IEEE Int. Symp. Pers. Indoor Mobile Radio Commun. (London, UK), 2013, pp. 332–336.
7. S. Chen et al., *Pattern division multiple access—a novel non-orthogonal multiple access for fifth-generation radio networks*, IEEE Trans. Veh. Technol. **66** (2017), no. 4, 3185–3196.
8. M. Al-Imari et al. *Performance evaluation of low density spreading multiple access*, in Proc. 8th Int, Wireless Commun. Mobile Comput. Conf. (Limassol, Cyprus), 2012, pp. 383–388.
9. D. Fang et al., *Lattice partition multiple access: a new method of downlink non-orthogonal multiuser transmissions*, in Proc. IEEE Global Commun. Conf. (Washington, DC, USA), 2016, pp. 1–6.
10. L. Dai et al., *Non-orthogonal multiple access for 5G: solutions, challenges, opportunities, and future research trends*, IEEE Commun. Mag. **53** (2015), no. 9, 74–81.
11. Z. Ding et al., *A survey on non-orthogonal multiple access for 5G networks: research challenges and future trends*, IEEE J. Sel. Areas Commun. **35** (2017), no. 10, 2181–2195.
12. Q. Li et al., *Index modulated OFDM spread spectrum*, IEEE Trans. Wireless Commun. **17** (2018), no. 4, 2360–2374.
13. T. Zeng et al., *Investigation on evolving single-carrier NOMA into multi-carrier NOMA in 5G*, IEEE Access **6** (2018), 48268–48288.
14. W. Cai et al., *Subcarrier and power allocation scheme for downlink OFDM-NOMA systems*, IET Signal Proc. **11** (2017), no. 1, 51–58.
15. T. A. Ayman and H. Arslan, *NOMA for multinumerology OFDM systems*, Wireless Commun. Mobile Comput. **2018** (2018), 1–9.
16. Y. Saito et al., *System-level performance evaluation of downlink non-orthogonal multiple access (NOMA)*, in Proc. IEEE Annu. Int. Symp. Personal, Indoor, Mobile Radio Commun. (London, UK), 2013, pp. 1–6.
17. Y. Sun et al. *Optimal joint power and subcarrier allocation for MC-NOMA systems*, in Proc. IEEE Global Commun. Conf. Washington, DC, USA, 2016, pp. 1–6.
18. Y. Sun et al., *Optimal joint power and subcarrier allocation for full duplex MC-NOMA systems*, IEEE Trans. Commun. **65** (2017), no. 3, 1077–1091.
19. Z. Ding, M. Peng, and H. V. Poor, *Cooperative non-orthogonal multiple access in 5G systems*, IEEE Commun. Lett. **18** (2015), no. 8, 1462–1465.
20. L. Lv et al., *Application of non-orthogonal multiple access in cooperative spectrum-sharing networks over nakagami-m fading channels*, IEEE Trans. Veh. Technol. **66** (2017), no. 6, 5506–5511.
21. D. T. Thai and P. Popovski, *Coordinated direct and relay transmission with interference cancelation in wireless systems*, IEEE Commun. Lett. **15** (2011), no. 4, 416–418.
22. D. T. Thai and M. Berbineau. Coordinated Direct and Relay Schemes for Two-Hop Communication in VANETS, 2014, Available from: https://arxiv.org/abs/1403.0173 [last accessed September 2019].
23. J. B. Kim et al., *System-level performance evaluation for non-orthogonal multiple access in coordinated direct and relay transmission*, in Proc. Int. Conf. Inf. Commun. Technol. Converg. (Jeju Island, Korea), 2017, pp. 1296–1298.
24. J. B. Kim and I. H. Lee, *Non-orthogonal multiple access in coordinated direct and relay transmission*, IEEE Commun. Lett. **19** (2015), no. 11, 2037–2040.
25. M. F. Kader and S. Y. Shin, *Coordinated direct and relay transmission using uplink NOMA*, IEEE Wireless Commun. Lett. **7** (2018), no. 3, 400–403.
26. L. Zheng et al., *On the performance of NOMA based coordinated direct and relay transmission using dynamic scheme*, IET Commun. **12** (2018), no. 18, 2231–2242.
27. N. T. Do et al., *A BNBF user selection scheme for NOMA-based cooperative relaying systems with swipt*, IEEE Commun. Lett. **21** (2017), no. 3, 664–667.
28. K. A. Shah and I. Koo, *A novel physical layer security scheme in OFDM-based cognitive radio networks*, IEEE Access **6** (2018), 29486–29498.
29. H. Khun, *The Hungarian method for the assignment problems*, Naval Res. Logistics Quarterly **62** (1995), no. 1–2, 83–97.
30. S. Haykin, *Cognitive radio: brain-empowered wireless communications*, IEEE J. Sel. Areas Commun. **23** (2015), no. 2, 202–220.
31. S. Zhang et al., *Novel spectrum sensing and access in cognitive radio networks*, Sci. China Inf. Sci. **61** (2018), no. 8, 089302.
32. Y. Liu et al., *Nonorthogonal multiple access in large-scale underlay cognitive radio networks*, IEEE Trans. Veh. Technol. **65** (2016), no. 12, 152–157.
33. N. Zabetian et al., *Rate optimization in NOMA cognitive radio networks*, in Proc. Int. Symp. Telecommun. (Tehran, Iran), 2016, pp. 62–65.

34. S. Arzykulov et al., *Outage performance of underlay CR-NOMA networks with detect-and-forward relaying*, in Proc. IEEE Global Commun. Conf. (Abu Dhabi, UAE), 2018, pp. 1–6.

35. G. Im and J. H. Lee, *Outage probability for cooperative NOMA systems with imperfect SIC in cognitive radio networks*, IEEE Commun. Lett. **23** (2019), no. 4, 692–695.

36. Y. Li, Z. Chen, and Y. Gong, *Optimal power allocation for coordinated transmission in cognitive radio networks*, in Proc. IEEE Veh. Technol. Conf. (Glasgow, UK), 2015, pp. 1–5.

37. M. F. Kader. A power-domain NOMA inspired overlay spectrum sharing scheme, 2018, Available from: https://engrxiv.org/vy3na/ [last accessed September 2019].

38. M. F. Kader and S. Y. Shin. *Cooperative spectrum sharing with space time bock Ccoding and non-orthogonal multiple access*, in Proc. Int. Conf. Ubiquitous Future Netw. (Vienna, Austria), 2016, pp. 490–494.

39. W. Xu et al., *Joint sensing duration adaptation, user matching, and power allocation for cognitive OFDM-NOMA systems*, IEEE Trans. Wireless Commun. **17** (2018), no. 2, 1269–1282.

40. Y. Sun, D. W. K. Ng, and R. Schober. *Resource allocation for MC-NOMA systems with cognitive relaying*, in Proc. IEEE Globecom Workshops (Singapore), 2017, pp. 1–7.

41. C. Li and X. Li. *Throughput maximization for multi-carrier non-orthogonal multiple access systems with coordinated direct and relay transmission*, in Proc. IEEE Int. Conf. Commun. (Kansas City, MO, USA), 2018, pp. 1–6.

42. M. Pischella and J. C. Belfiore, *Weighted sum throughput maximization in multicell OFDMA networks*, IEEE Trans. Veh. Technol. **59** (2010), no. 2, 896–905.

43. G. De Angelis, G. Baruffa, and S. Cacopardi, *Gnss/cellular hybrid positioning system for mobile users in urban scenarios*, IEEE Trans. Intell. Transp. Syst. **14** (2013), no. 1, 313–321.

44. K. Kyamakya and K. Jobmann, *Location management in cellular networks: classification of the most important paradigms, realistic simulation framework, and relative performance analysis*, IEEE Trans. Veh. Technol. **54** (2005), no. 2, 687–708.

45. S. Boyd, Convex optimization (7th ed.), Cambridge University Press, Cambridge, UK, 2009.

46. S. Boyd. Lecture on class ee364b of Stanford University, 2017, Available from: http://www.stanford.edu/class/ee364b/lectures.html [last accessed September 2019].

47. A. Benjebbour et al., *System-level performance of downlink NOMA for future LTE enhancements*, in Proc. IEEE Globecom Workshops (Atlanta, GA, USA), 2013, pp. 66–70.

48. Z. Yang et al., *The impact of power allocation on cooperative non-orthogonal multiple access networks with SWIPT*, IEEE Trans. Wireless Commun. **16** (2017), no. 7, 4332–4343.

49. Y. Yuan et al., *Energy efficiency optimization in full-duplex user-aided cooperative SWIPT NOMA systems*, IEEE Trans. Commun. **65** (2019), no. 6, 2641–2656.

AUTHOR BIOGRAPHIES

Thirunavukkarasu Manimekalai received her BE degree in electronics and communication engineering from the University of Madras, Chennai, India, in 1994, and her ME degree in optical communication and PhD degree from Anna University, Chennai, in 2001 and 2013, respectively. She is currently a faculty member in the Department of Electronics and Communication Engineering, College of Engineering, Guindy, Anna University. She has authored works in international journals and conferences. Her research interests include physical and cross-layer designs in wireless communication and networking—cognitive radio, non-orthogonal multiple access, and cooperative communication.

Sparjan Romera Joan received her BE degree in electronics and communication engineering from Anna University, Chennai, India, in 2016, and her ME degree in communication systems from the College of Engineering, Guindy, Anna University, in 2019. She is currently a research scholar with the College of Engineering, Guindy, Anna University. Her current research interests include next-generation wireless communication networks.

Thangavelu Laxmikandan received his BE degree in electronics and communication engineering from the University of Madras, Chennai, India, his MTech degree in communication systems from the Indian Institute of Technology Madras, Chennai, and his PhD degree from Anna University, Chennai, in 2000, 2002, and 2015, respectively. He is a recipient of the EFIP-2000 fellowship during his post-graduation. He is currently an associate professor with the College of Engineering, Guindy, Anna University. He has authored works in international conferences and publications. His current research interests include system modeling and design for wireless communication and networks.